Analysis and simulation of a coupled-cavity pulse compressor

XIAO Ou-Zheng(肖欧正) ZHAO Feng-Li(赵风利)

Institute of High Energy Physics, Chinese Academy of Sciences, Beijing 100049, China

Abstract: An equivalent circuit model is built for a coupled-resonator pulse compressor. Based on the circuit, the general second order differential equation is derived and converted into the first order equation to save computing time. In order to analyze the transient response and optimize parameters for the pulse compressor, we have developed a simulation code. In addition, we have also designed a three-cavity pulse compressor to get the maximum energy multiplication factor. The size of the cavities and coupling apertures is determined by HFSS.

Key words: pulse compressor, power gain, energy multiplication factor

PACS: 29.20.-c **DOI:** 10.1088/1674-1137/36/11/017

1 Introduction

In the 1990s, the coupled-cavity pulse compressor was first proposed by T. Shintake, who also fabricated a cold model and got reasonable results [1, 2]. It can produce a flatter output waveform than that of the SLED (SLAC Energy Doubler). Although dispersion distorts the waveform and gives rise to a significant power variation in the compressed pulse, its physical length is much shorter than that of the SLED Ⅱ. Theoretical analysis and numerical simulation for a coupled-cavity pulse compressor will be presented.

2 Transient analysis [3, 4]

The coupled-cavity pulse compressor is studied using the coupled-resonator model which has been successfully applied to analyze the characteristics of the accelerating structures. Fig. 1 shows the equivalent circuit of the pulse compressor.

The characteristic impendence of the feeding waveguide is normalized to 1. Each cavity is represented by a parallel resonant circuit. The coefficient k describes the coupling between the two adjacent cavities and β is the coupling between the feeding waveguide and the first cavity. Based on the equivalent circuit, the general differential equation can be obtained as Eq. (1). Assuming that the voltages oscillate with a sinusoidal function at the frequency ω, then Eq. (1) can be transformed into Eq. (2).

$$\begin{aligned}
&\frac{\mathrm{d}^2v_1}{\mathrm{d}t^2}+\frac{w_1(1+\beta)}{Q_1}\frac{\mathrm{d}v_1}{\mathrm{d}t}+w_1^2v_1\\
&=\frac{1}{2}k_{1,2}w_1w_2v_2+\frac{2w_1\beta}{Q_1}\frac{\mathrm{d}v_\mathrm{g}}{\mathrm{d}t},\\
&\frac{\mathrm{d}^2v_n}{\mathrm{d}t^2}+\frac{w_n}{Q_n}\frac{dv_n}{\mathrm{d}t}+w_n^2v_n\\
&=\frac{1}{2}k_{n-1,n}w_{n-1}w_nv_{n-1}\\
&\quad+\frac{1}{2}k_{n,n+1}w_nw_{n+1}v_{n+1},(2\leqslant n\leqslant N-1)\\
&\frac{\mathrm{d}^2v_N}{\mathrm{d}t^2}+\frac{w_N}{Q_N}\frac{\mathrm{d}v_N}{\mathrm{d}t}+w_N^2v_N\\
&=\frac{1}{2}k_{N-1,N}w_{N-1}w_Nv_{N-1},
\end{aligned}\tag{1}$$

Received 11 January 2012

$$\frac{\mathrm{d}^2V_1}{\mathrm{d}t^2}+\left(\mathrm{j}2w+\frac{w_1(1+\beta)}{Q_1}\right)\frac{\mathrm{d}V_1}{\mathrm{d}t}+\left(w_1^2-w^2+\frac{\mathrm{j}ww_1(1+\beta)}{Q_1}\right)V_1$$

$$=\frac{1}{2}k_{1,2}w_1w_2V_2+\frac{2w_1\beta}{Q_1}\frac{\mathrm{d}V_\mathrm{g}}{\mathrm{d}t}+\frac{\mathrm{j}2ww_1\beta}{Q_1}V_\mathrm{g},$$

$$\frac{\mathrm{d}^2V_n}{\mathrm{d}t^2}+\left(\mathrm{j}2w+\frac{w_n}{Q_n}\right)\frac{\mathrm{d}V_n}{\mathrm{d}t}+\left(w_n^2-w^2+\frac{\mathrm{j}ww_n}{Q_n}\right)V_n$$

$$=\frac{1}{2}k_{n-1,n}w_{n-1}w_nV_{n-1}+\frac{1}{2}k_{n,n+1}w_nw_{n+1}V_{n+1},(2\leqslant n\leqslant N-1),$$

$$\frac{\mathrm{d}^2V_N}{\mathrm{d}t^2}+\left(\mathrm{j}2w+\frac{w_N}{Q_N}\right)\frac{\mathrm{d}V_N}{\mathrm{d}t}+\left(w_N^2-w^2+\frac{\mathrm{j}ww_N}{Q_N}\right)V_N=\frac{1}{2}k_{N-1,N}w_{N-1}w_NV_{N-1}. \quad (2)$$

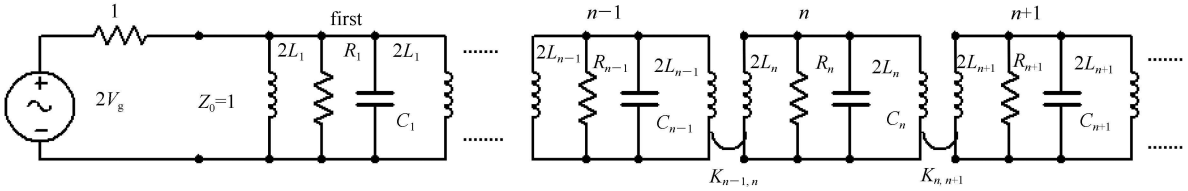

Fig. 1. Equivalent circuit for the coupled-cavity pulse compressor.

If the amplitude of the excitation source varies smoothly and the cavities have a high quality factor, the second order equation can be approximated as the first order equation.

$$2\frac{\mathrm{d}V_1}{\mathrm{d}t}+\frac{w(1+\beta)}{Q_1}V_1=-\mathrm{j}\frac{1}{2}k_{1,2}wV_2+\frac{2w\beta}{Q_1}V_\mathrm{g},$$

$$2\frac{\mathrm{d}V_n}{\mathrm{d}t}+\frac{w}{Q_n}V_n=-\mathrm{j}\frac{1}{2}w(k_{n-1,n}V_{n-1}+k_{n,n+1}V_{n+1}),(2\leqslant n\leqslant N-1)$$

$$2\frac{\mathrm{d}V_N}{\mathrm{d}t}+\frac{w}{Q_N}V_N=-\mathrm{j}\frac{1}{2}k_{N-1,N}wV_{N-1}, \quad (3)$$

Eqs. (2) and (3) are solved for the three-cavity system with Q factor of 190000. And the generator frequency is 5.712 GHz, which is the same as the resonant frequency of cavities. The duration of the input pulse is 2.5 μs and that of the output pulse is 0.35 μs. Fig. 2 shows the results of Eq. (2) solved by the Runge-Kutta method and that of Eq. (3) solved directly when the power gain is maximized. It shows that the results are almost entirely consistent, that is to say, the first-order approximation is reasonable.

Tables 1 and 2 show the optimum parameters of uniform coupled-cavity systems with a Q factor of 190000 when the power gain and M are maximized, respectively. Fig. 3 shows the normalized power gains using the parameters in Table 1. Fig. 4 shows the normalized voltages using the parameters in Table 2. In this case, it can be concluded that the quantity of the cavity has little effect on the maximum power gain and energy multiplication factor, but the output waveform is flatter with the increase of it.

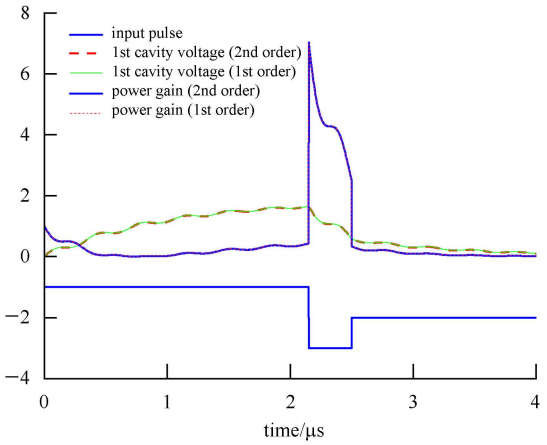

Fig. 2. The output waveform of Eqs. (1) and (2) when the power gain is maximized.

Table 1. The optimum parameters with maximum power gain.

quantity	β	k	power gain	efficiency(%)
3	20.6	0.0014	4.37	61
5	30.8	0.00205	4.36	61
7	41	0.00265	4.35	60.9
9	51.2	0.00325	4.35	60.9

Furthermore, with different Q factor and k, the nonuniform three-cavity system is analyzed. Fig. 5 shows the parameters and output waveform when M

Table 2. The optimum parameters with maximum multiplication factor.

quantity	β	k	M
3	19.1	0.0013	2.037
5	29	0.00185	2.047
7	39.3	0.0025	2.054
9	49	0.003	2.057

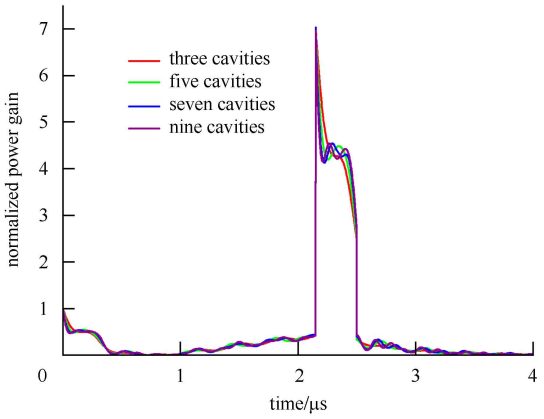

Fig. 3. The output waveform of the normalized power gain.

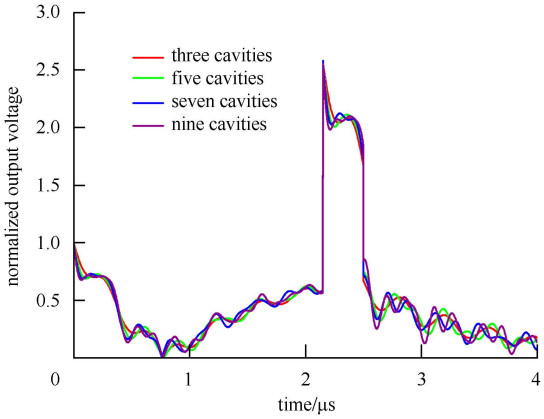

Fig. 4. The output waveform of the normalized voltage.

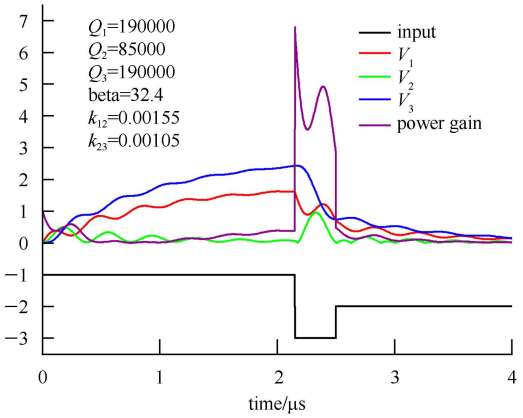

Fig. 5. Output waveform of the nonuniform three-cavity system.

is maximized to 2.06, and then the power gain is 4.33, very close to the maximum value of 4.35.

3 Results of simulation by HFSS

Three-dimensional field calculations have been carried out by HFSS to determine the size of coupling apertures and cavities. The relation between k and frequency in a dual-cavity system can be expressed as [5]

$$k = 2\sqrt{\frac{[(f_{02}^2/f_1^2)-1][(1-f_{01}^2/f_2^2)]}{f_{01}^2/f_1^2+f_{01}^2/f_2^2-1}}, \tag{4}$$

where f_1 and f_2 are the eigenmode frequency of the dual-cavity system, f_{01} and f_{02} are the frequency of the two single-cavity. We split the three-cavity system into two dual-cavity systems to get k_{12} and k_{23}, respectively. Tables 3 and 4 show the simulation results of the coupling coefficients.

The steady-state equation of the coupled-resonator modal can be obtained by Fourier transform of Eq. (1). Analyzing steadythe -state response of the three-cavity system, we get three eigenmodes: 0, $\pi/2$ and π modes. Their frequencies can be expressed as:

$$\begin{aligned} w_{\pi/2} &= w_1 = w_2 = w_3 = w, \\ w_{\pi or 0} &= \frac{w}{\sqrt{1 \pm \frac{1}{2}\sqrt{k_{12}^2+k_{23}^2}}}. \end{aligned} \tag{5}$$

The $\pi/2$ mode is chosen as the operating mode for its stabilization, which can relax the requirements for machining tolerances. Figs. 6, 7 and 8 show the magnetic field pattern of 0, $\pi/2$ and π modes of the three-cavity pulse compressor. Fig. 9 shows the detailed size of the pulse compressor.

Theoretically there are three ways to verify the reliability and accuracy of the simulation results. First of all, we compare the frequency of the three eigenmodes simulated by HFSS with that solved by Eq. (5). The results are showed in Table 5. Secondly, we can compare f_{02} obtained by HFSS with that calculated with Eq. (6). Lastly, we compute the ratio of stored energy in the first and third cavities by HFSS which is equal to the square of the ratio of k_{23} and k_{12}. The results of simulation and theoretical calculation are consistent.

$$f_{02} = \frac{f_{01}}{\sqrt{f_{01}^2/f_1^2+f_{01}^2/f_2^2-1}}. \tag{6}$$

Table 3. The simulation results of k_{12}.

1st cavity frequency	2nd cavity frequency	0 mode frequency	π mode frequency	k_{12}
5712.02 MHz	5712.06 MHz	5709.88 MHz	5714.18 MHz	0.0015

Table 4. The simulation results of k_{23}.

2nd cavity frequency	3th cavity frequency	0 mode frequency	π mode frequency	k_{23}
5712.06 MHz	5711.98 MHz	5710.6 MHz	5713.48 MHz	0.001

Table 5. The frequency of 0, π/2 and π modes.

mode	0 Mode	π/2 mode	π mode
frequency by HFSS	5709.46 MHz	5712.03 MHz	571463 MHz
frequency by Eq. (5)	5709.46 MHz	5.712.03 GHz	5714.61 MHz

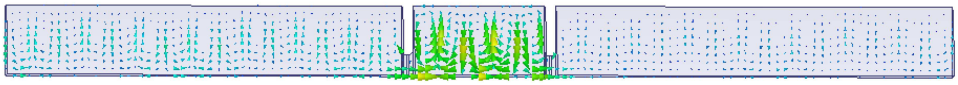

Fig. 6. The magnetic field pattern of 0 mode.

Fig. 7. The magnetic field pattern of π/2 mode.

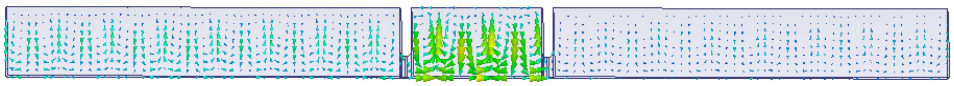

Fig. 8. The magnetic field pattern of π mode.

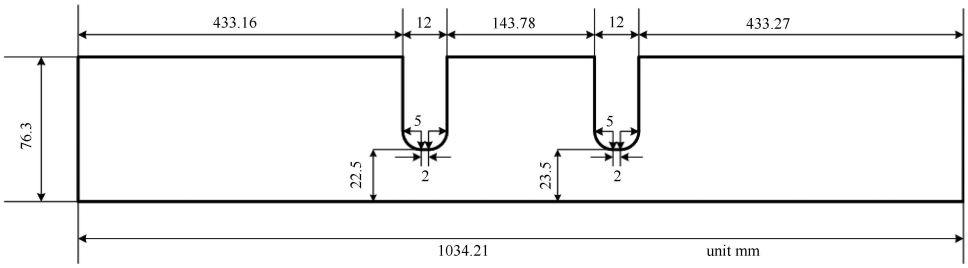

Fig. 9. The size of coupling aperture and cavities.

4 Conclusion

We have described the complete theoretical analysis of the coupled-cavity pulse compressor and optimize the parameters under different conditions. In addition, we have designed a coupled-cavity RF pulse compressor similar to that proposed by T. Shitake and simulated it by HFSS. The cavity size is determined in the case of the eigenmode. After the introduction of the input coupler, just fine-tuning for the input cavity size is needed. The results can be used as a useful reference for future design and manufacture.

References

1 Shitake T, Akasaka N. A New Rf Pulse Compressor Using Multi-cell Coupled-Cavity System. Proc. of EPAC. Barcelona, 1996. 2146–2148

2 Shintake T, Akasaka N, Matsumoto H. Development of C-band RF Pulse Compression System for e^+e^- Linear Collider. Proc. of the 17th IEEE Conf. on Particle Accelerator. Vancouver, 1997. 455–457

3 Nantista C D. Radio-Frequency Pulse Compression for Linear Accelerators. SLAC-R-95-455. 1995

4 Fiebig A, Schieblich Ch. A SLED Type Pulse Compressor with Rectangular Pulse Shape. CERN-PS-90-13-RF. 1990

5 BIAN Xiao-Hao, CHEN Huai-Bi, ZHENG Shu-Xin. HEP & NP, 2006, **30**(01): 62–65 (in Chinese)